Available online at www.sciencedirect.com
SCIENCE DIRECT®
Journal of Power Sources 147 (2005) 1–7
JOURNAL OF POWER SOURCES
www.elsevier.com/locate/jpowsour

Performance and electrode behaviour of nano-YSZ impregnated nickel anodes used in solid oxide fuel cells

S.P. Jiang *, W. Wang, Y.D. Zhen

Fuel Cells Strategic Research Program, School of Mechanical and Production Engineering, Nanyang Technological University, Nanyang Avenue, Singapore 639798, Singapore

Received 8 October 2004; accepted 28 December 2004
Available online 26 February 2005

Abstract

The effect of impregnation of nano-sized Y_2O_3–ZrO_2 (YSZ) particles into nickel anodes on the performance and electrode behaviour for the hydrogen oxidation reaction is investigated. Incorporation of nano-YSZ particles significantly reduces the electrode polarization resistance and overpotentials for the hydrogen oxidation reaction. Furthermore, the electrode behaviour for the hydrogen oxidation reaction on the nano-YSZ impregnated nickel anode is clearly differentiated at low and high frequencies. Impregnation of nano-YSZ particles primarily decreases the electrode polarization resistance at high frequencies, which indicates that the main role of the impregnated YSZ is to extend the three-phase boundary areas into the bulk of the nickel anode. The results suggest that the electrode process at low frequencies may be dominated by the dissociative adsorption of hydrogen.

Keywords: Solid oxide fuel cells; Nickel anodes; Nano-YSZ; Ion impregnation; Hydrogen oxidation reaction

1. Introduction

In a thin electrolyte solid oxide fuel cell (SOFC), operating at intermediate temperatures of 600–800 °C, the overall cell losses are dominated by the electrode reactions at the electrode and electrolyte interfaces due to the significant reduction in the electrolyte thickness [1]. Thus, development of electrode materials with high performance and stability is important for the commercial viability of the SOFC technologies. This can be achieved either by development of new electrode materials with high mixed ionic and electronic conductivity (MIEC), or by continuous modification/improvement of existing electrode materials developed for high-temperature operations (typically at 1000 °C), such as Sr-doped $LaMnO_3$ cathodes and Ni/Y_2O_3–ZrO_2 (Ni/YSZ) cermet anodes. The advantages of the existing electrode materials are their proven electrocatalytic activity at high temperatures and good stability with YSZ electrolyte materials.

Ni/YSZ-based cermets are still the most common anode materials used in SOFCs due to the excellent electrocatalytic activity for the hydrogen oxidation reaction, high electrical conductivity and high stability and compatibility with the Y_2O_3–ZrO_2 (YSZ) electrolyte [2]. As shown recently by Bieberle et al. [3], the electrocatalytic activities of nickel anodes for the hydrogen oxidation are directly related to the length of the three-phase boundary (TPB) where nickel, YSZ and hydrogen gas meet. This indicates that the size and distribution of the nickel and YSZ phases in the Ni/YSZ cermets are critical to the performance of cermet anodes [4–6]. Conventional Ni/YSZ cermet anodes are usually prepared by using commercial NiO and YSZ powders and are homogenized by a ceramic mixing process [5]. It has been shown, however, that high temperature sintering (∼1400 °C) and reducing (∼1000 °C) steps associated with the conventional Ni/YSZ fabrication process cause significant grain growth of both the nickel and the YSZ phases in the cermet [7]. On the other hand, ion impregnation has been found to be an effective method for introducing nano-sized ionic conducting oxide particles into the SOFC electrode structure due to the

* Corresponding author. Tel.: +65 6790 5010; fax: +65 6791 1859.
E-mail address: mspjiang@ntu.edu.sg (S.P. Jiang).

0378-7753/$ – see front matter © 2005 Elsevier B.V. All rights reserved.
doi:10.1016/j.jpowsour.2004.12.042

much lower heat-treatment temperature of the process [7–10]. In this paper, the effect of the impregnation of nano-YSZ on the performance and electrode behaviour of pure nickel anodes is investigated. The results indicate that this procedure not only substantially enhances the performance of the anodes but also significantly influences the electrode behaviour of the anode for hydrogen oxidation.

2. Experimental

Electrolyte substrates were prepared by dry pressing 8 mol% Y_2O_3–ZrO_2 powder (TZ8Y, Tosoh, Japan), followed by sintering at 1500 °C for 4 h in air. The electrolyte thickness and diameter were 1 and 19 mm, respectively. NiO (J.T. Baker) powders were pre-coarsened at 600 °C for 2 h in air to reduce powder shrinkage and to improve coating quality [5]. The powder was ball-milled in propanol for 5 h, using TZ3Y balls (Tosoh, Japan) as the milling medium. A NiO electrode ink was prepared using polyethylenglycol and applied to the YSZ electrolyte by slurry painting. The anodes were sintered at 1400 °C for 2 h and the electrode area was 0.5 cm^2. A three-electrode system was used for electrochemical measurements. Platinum paste was painted on the reverse of the working electrode to make counter and reference electrodes. The counter electrode was positioned symmetrically to the working electrode and a reference electrode was painted as a ring around the counter electrode. The gap between the counter and reference electrodes was ∼4 mm. Hydrogen gas humidified at room temperature (∼3% H_2O) was used as the fuel and air was used as the oxidant. NiO was reduced in situ under the hydrogen fuel environment. The electrochemical performance of the nickel anodes was characterized by polarization and electrochemical impedance spectroscopy (EIS) techniques. The latter was performed with a Solartron 1260 impedance/gain phase analyzer in conjunction with a Solartron 1287 electrochemical interface. The frequency range was from 0.1 Hz to 1 MHz with an amplitude of 10 mV. Impedance responses were analyzed using the equivalent circuit fitting program of Z-plot. The electrode performance of the pure and impregnated nickel anodes for the H_2 oxidation reaction was measured generally at 700–900 °C.

A nano-YSZ suspension (NexTech, USA) was used for the ion impregnation of the nickel anodes. A dropper was used to deposit the solution on the top surface of the nickel anodes and the solution was allowed to soak into the porous structure of the anode in open air. The surface of the electrode coating was wiped with a soft tissue and dried in open air. The impregnated sample was heat treated at 850 °C for 1 h to decompose the organic components of the suspension. The loading of the impregnated oxides was estimated by measuring the weight before and after the impregnation treatment. The impregnation treatment was repeated to increase the loading of the oxide phase. The thickness of the anode was measured using a TalyScan 150 dual-gauge system (Taylor Hobson) and the microstructure was examined with a scanning electron microscope (SEM; Leica S360). The porosity of the anode was estimated by SEM image analysis of the anodes [11]. Based on the electrode thickness and porosity, the volume percentage of the impregnated YSZ in the Ni anode can be calculated [10].

3. Results and discussion

3.1. Microstructure

The YSZ loading of the impregnated Ni anodes was 2.7 mg cm^{-2} after one impregnation treatment and 4.0 mg cm^{-2} after repeated impregnation treatment. From image analysis of scanning electron micrographs of the electrode cross-section, the porosity of the nickel anode coating was found to be ∼30%. The coating thickness was in the range of 20–38 μm. Thus, the volume percentage of the impregnated YSZ in the anode was 17 vol.% after one impregnation and 21 vol.% after repeated impregnation. The volume percentage of the YSZ phase in the nano-YSZ impregnated nickel anodes is far below the 50 vol.% that is typically used in the conventional Ni/YSZ cermet anodes [5,7].

Scanning electron micrographs of the surface and fractured cross-sections of pure nickel and nano-YSZ impregnated nickel anodes with a YSZ loading of 2.7 mg cm^{-2} are

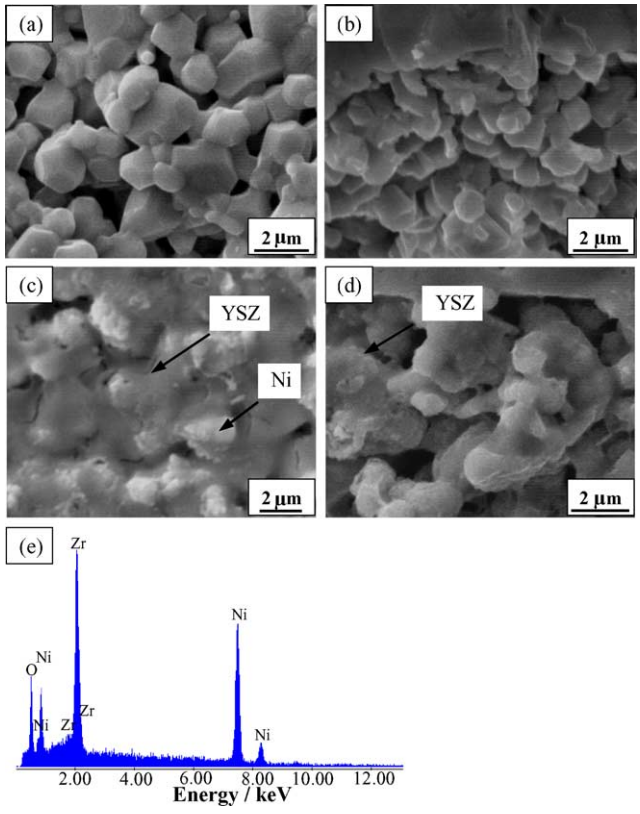

Fig. 1. Scanning electron micrographs of: (a) surface; (b) fractured cross-section of pure nickel; (c) surface; (d) fractured cross-section of 2.7 mg cm^{-2} nano-YSZ impregnated nickel anode and (e) EDS of YSZ-covered nickel particles of (c).

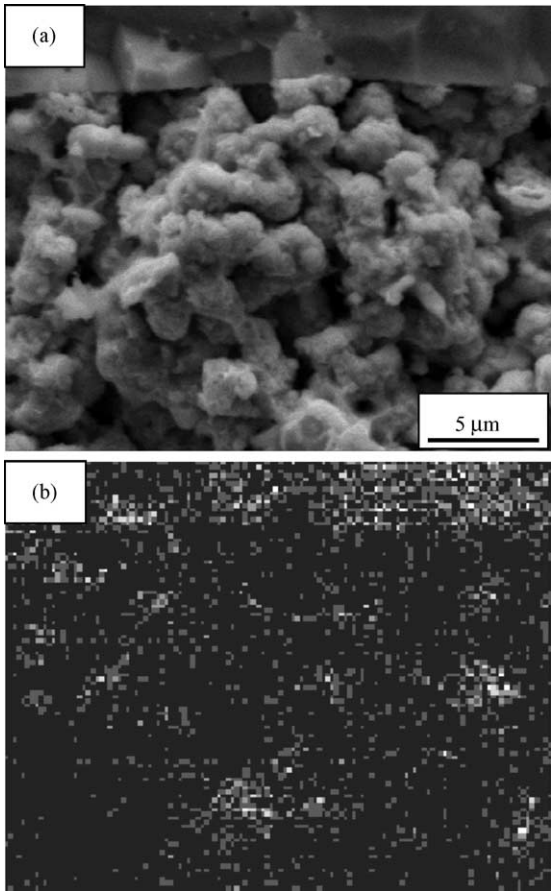

Fig. 2. (a) Scanning electron micrograph picture and (b) Zirconium element mapping of a 4.0 mg cm^{-2} nano-YSZ impregnated nickel anode.

presented in Fig. 1. For pure nickel anodes, the particle size is 1.6 ± 0.48 μm. After one impregnation treatment with a YSZ loading of 2.7 mg cm^{-2}, there is clearly the formation of thin oxide films on the surface of the particles (Fig. 1c and d). Nevertheless, there is no visible change in the size of the particles. EDS analysis of the nano-YSZ covered nickel particles indicates that the thin film is most likely composed of a Y_2O_3–ZrO_2 oxide phase (Fig. 1e). It appears that there are more YSZ particles precipitated on the nickel anode surface as compared to that inside the anode. This is also indicated by the formation of a denser layer on the surface of the 4.0 mg cm^{-2} nano-YSZ impregnated Ni anode. Thus, the actual loading of impregnated YSZ inside the anode would be smaller than that calculated.

Fig. 2 shows the SEM picture of the fractured cross-section of a 4.0 mg cm^{-2} YSZ impregnated Ni anode and the corresponding Zr mapping. As indicated by the Zr mapping (Fig. 2b), YSZ was uniformly distributed inside the nickel anode. The particle size of the YSZ phase in the impregnated nickel anodes is estimated from the enlarged SEM images to be in the range 100–300 nm. In the case of the Ni/YSZ cermet anodes prepared by the conventional ceramic mixing and sintering process, the YSZ particles in the cermet are typically in the range of 1–3 μm [5,12]. The nano-sized YSZ in the impregnated Ni anodes is clearly due to the much lower heat-treatment temperature (∼850 °C) of the process as compared with the anode sintering temperature of ∼1400 °C used in the conventional fabrication process. The uniform and discrete distribution of the nano-YSZ particles inside the porous structure of nickel anodes demonstrates that impregnation is an effective method for introducing an electrocatalytic phase into the electrodes of solid oxide fuel cells.

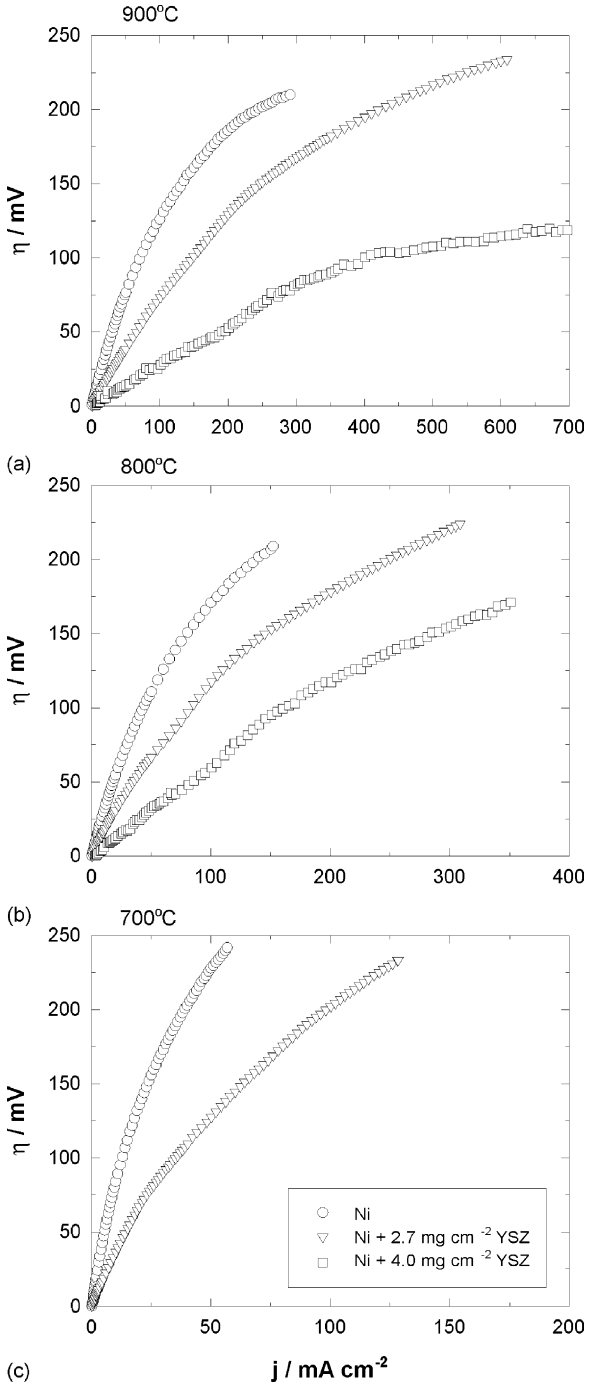

Fig. 3. Polarization performance of H_2 oxidation reaction on pure nickel, 2.7 mg cm^{-2} and 4.0 mg cm^{-2} nano-YSZ impregnated nickel anodes at different temperatures.

3.2. Electrode performance

The polarization performance of the hydrogen oxidation reaction on pure, 2.7 mg cm^{-2} and 4.0 mg cm^{-2} nano-YSZ impregnated Ni anodes at different temperature is presented in Fig. 3. With nano-YSZ impregnation, the polarization losses for the reaction are substantially reduced. At 900 °C, the overpotential (η) for the reaction on the pure nickel anode is 195 mV at 200 mA cm^{-2}. With 2.7 and 4.0 mg cm^{-2} nano-YSZ impregnation, η is reduced to 130 and 63 mV, respectively, under the same current conditions. Similar improvements in the electrode polarization performance is observed at other temperatures (Fig. 3b and c).

The significant enhancement of the electrode polarization performance of the impregnated nickel anodes compared with that of pure Ni anodes is also confirmed by the electrode impedance behaviour. Nyquist and Bode plots for hydrogen oxidation on pure and nano-YSZ impregnated nickel anodes at different temperatures in 97% H_2/3% H_2O are shown in Fig. 4. The impedance curves were measured under open-circuit conditions. The equivalent circuit for the analysis of the impedance data is illustrated in Fig. 5. The symbols represent the measured data and the solid lines are the fitted data. Good agreement is found between the equivalent circuit and the observed impedance data, which indicates the reasonability of the choice of equivalent circuit. The fitted impedance parameters for hydrogen oxidation on pure and impregnated Ni anodes at different temperatures are given in Table 1.

For the hydrogen oxidation reaction on pure nickel anodes, the impedance responses are characterized by a very large and depressed arc and the hydrogen oxidation reaction

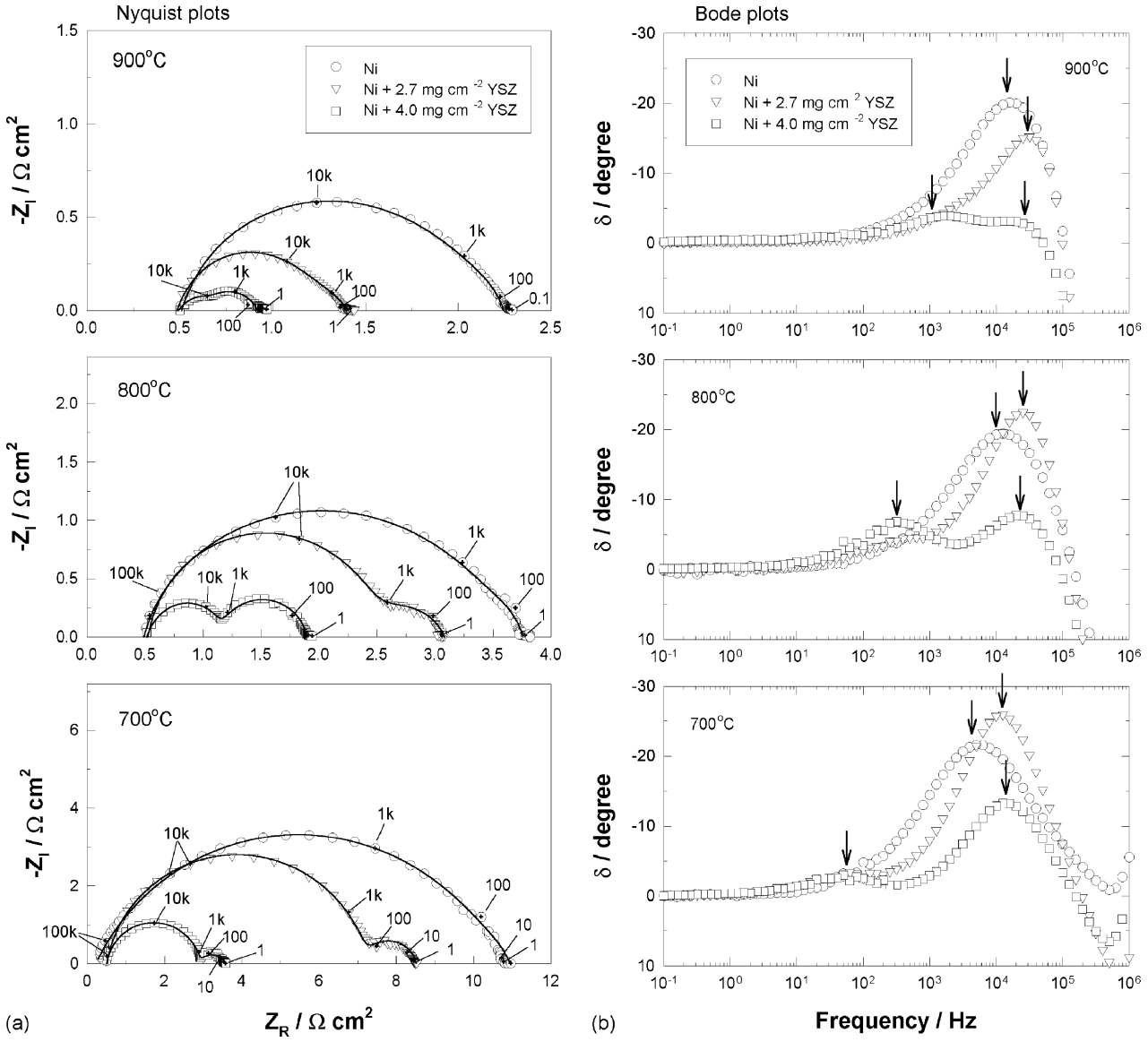

Fig. 4. (a) Nyquist and (b) Bode plots for hydrogen oxidation on pure and nano-YSZ impregnated nickel anodes at different temperatures. Symbols are experimental data and solid lines are fitted impedance data. Numbers are frequency in Hz.

Table 1
Fitted impedance parameters for hydrogen oxidation on nickel and nano-YSZ impregnated nickel anodes

Electrode	Temperature (°C)	Low-frequency arc			High-frequency arc		
		$R_{E,L}$ ($\Omega\,cm^2$)	Q_L ($F\,cm^{-2}$)	n	$R_{E,H}$ ($\Omega\,cm^2$)	Q_H ($F\,cm^{-2}$)	n
Ni	900	0.13	2.99×10^{-3}	0.9	1.75	6.23×10^{-5}	0.8
	800	0.18	1.71×10^{-3}	1.0	3.25	5.43×10^{-5}	0.8
	700	0.31	1.00×10^{-2}	0.9	10.41	4.83×10^{-5}	0.7
2.7 mg cm^{-2} YSZ + Ni	900	0.34	3.08×10^{-3}	0.6	0.66	8.58×10^{-6}	0.9
	800	0.61	2.66×10^{-3}	0.8	2.02	5.95×10^{-6}	0.9
	700	1.26	4.76×10^{-3}	0.8	6.81	7.02×10^{-6}	0.9
4.0 mg cm^{-2} YSZ + Ni	900	0.29	2.05×10^{-3}	0.8	0.24	1.03×10^{-5}	1.0
	800	0.48	4.04×10^{-3}	0.8	0.71	8.37×10^{-6}	1.0
	700	0.65	2.09×10^{-2}	0.7	2.46	8.15×10^{-6}	0.9

is dominated by the electrode processes at high frequencies. After nano-YSZ impregnation, the overall impedance arcs are reduced significantly. For hydrogen oxidation on the pure nickel anode, the overall electrode polarization or interface resistance (R_E) is 1.9, 3.3 and 10.7 $\Omega\,cm^2$ at 900, 800 and 700 °C, respectively. With the impregnation of 4.0 mg cm^{-2} nano-YSZ, R_E is reduced to 0.5, 1.4 and 3.1 $\Omega\,cm^2$, respectively, at the corresponding temperatures. Thus, the electrode resistance is reduced by three to four times for the reaction on 4.0 mg cm^{-2} nano-YSZ impregnated nickel anodes with respect to the pure nickel anode. Moreover, impregnation of the nano-YSZ phase on nickel anodes appears to have a greater enhancing effect on the reduction of the electrode polarization resistance at high frequencies than that at low frequencies. As shown early, hydrogen oxidation on nickel anodes at high frequencies is most likely related to the charge-transfer reaction at the electrode|electrolyte three-phase boundary (TPB) region [13]. This indicates that impregnation of the nano-sized YSZ phase mainly increases the electrochemical reaction sites for H_2 oxidation reactions by extending the TPB into the bulk of the Ni anodes.

In addition to significant reduction in the electrode polarization resistance, there is a significant change in the distribution of low- and high-frequency arcs for the reaction on the nano-YSZ impregnated Ni anodes. The electrode processes are clearly separable and are differentiated at low and high frequencies, as indicated by the appearance of two characteristic frequencies on the Bode plots (arrows in Fig. 4b). For hydrogen oxidation on pure Ni anodes, there is only one dominant electrode process associated with the high-frequency arc and its characteristic frequency is ~10 kHz. Impregnation of the nano-YSZ phase increases slightly this characteristic frequency to ~30 kHz, and the electrode process associated with the low-frequency arc becomes increasingly visible and important. The characteristic frequency of the electrode process at the low-frequency arc is 1000 Hz at 900 °C and decreases to ~60 Hz as the temperature is decreased to 700 °C (Fig. 4b). In contrast to the behaviour of the high-frequency arc, impregnation of nano-YSZ phase has no effect on the characteristic frequency of the low-frequency arc. In general, these are two orders of difference in the magnitude of the characteristic frequency for the electrode processes at low- and high-frequencies.

The effect of YSZ loading on the electrode polarization resistance at the low- and high-frequency arcs ($R_{E,H}$ and $R_{E,L}$) at different temperatures is shown in Fig. 6. The open symbols present $R_{E,H}$ and the solid symbols $R_{E,L}$. Impregnation of nano-YSZ particles in Ni anodes substantially decreases the value of $R_{E,H}$, whereas the effect on $R_{E,L}$ is very much smaller. This shows that the impregnated particles have a differential catalytic effect on hydrogen oxidation at high- and low-frequencies. This differential effect separates the elec-

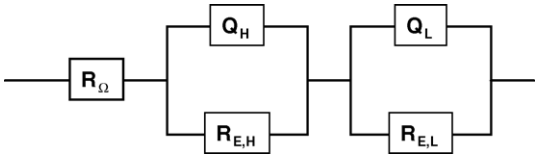

Fig. 5. Equivalent circuit for fitting of impedance data of hydrogen oxidation on nickel and nano-YSZ impregnated nickel anodes. In the circuit, R_Ω is electrolyte resistance, Q the constant-phase element or CPE, R_E the electrode polarization resistance, and subscript H and L refer to high- and low-frequency arcs, respectively.

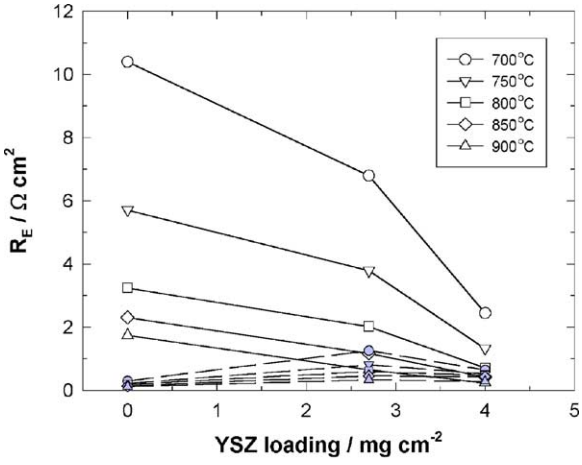

Fig. 6. Dependence of electrode polarization resistance of low- and high-frequency arcs ($R_{E,H}$ and $R_{E,L}$) on impregnated YSZ loading at different temperatures. Open symbols present $R_{E,H}$ and solid symbols $R_{E,L}$.

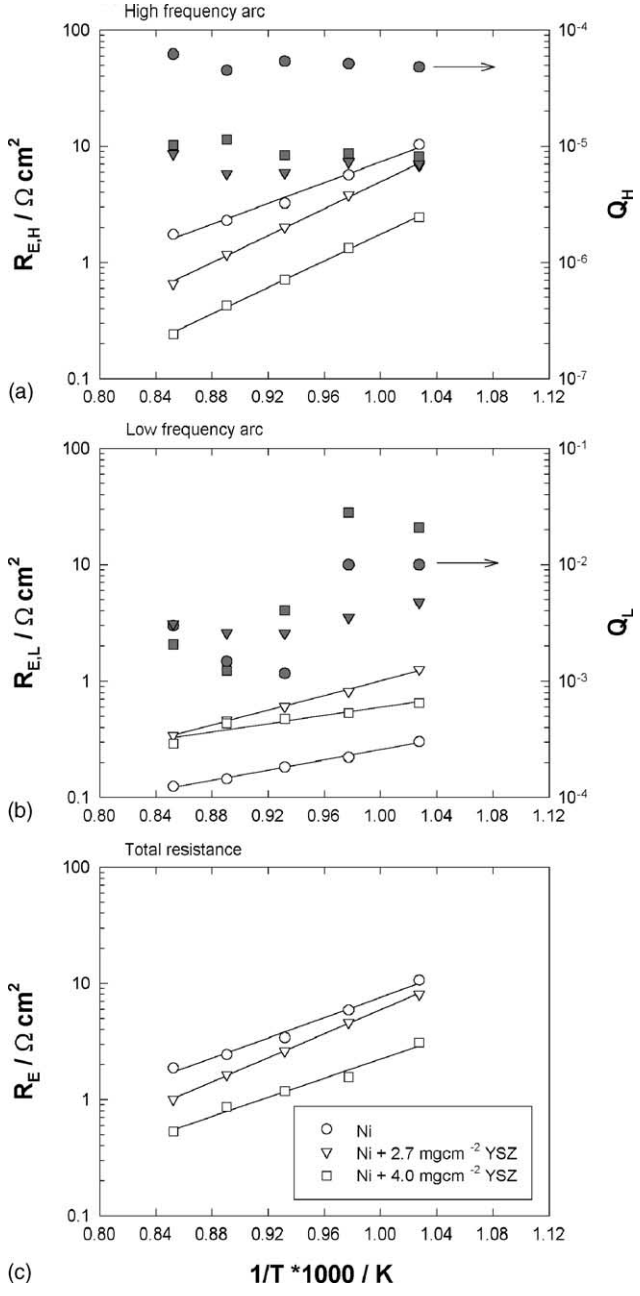

Fig. 7. Activation energy plots of electrode polarization resistance of low- and high-frequency arcs (R_L and R_H, empty symbols) and constant-phase element (Q_H and Q_L, solid symbols) for hydrogen oxidation on pure and nano-YSZ impregnated nickel anodes.

trode processes and reduces the ambiguousness in the interpretation and, in particular, in the equivalent circuit analysis of the electrode impedance responses.

Activation energy plots of the electrode polarization resistance (R_L and R_H) and the constant-phase element (Q_H and Q_L) of low- and high-frequency arcs for the reaction on pure and nano-YSZ impregnated Ni anodes are presented in Fig. 7. The activation energies of the total and the electrode polarization resistance for the reaction at low- and high-frequency arcs are summarized in Table 2. Clearly, impregnation of the

Table 2
Activation energy of total electrode polarization resistance and electrode polarization resistance of low- and high-frequency arcs

Electrode	Activation energy (kJ mol^{-1})		
	Low-frequency arc	High-frequency arc	Total
Ni	42	85	84
2.7 mg cm^{-2} YSZ + Ni	57	111	99
4.0 mg cm^{-2} YSZ + Ni	35	110	79
	46 ± 9	102 ± 12	87 ± 8

nano-YSZ phase has little influence on the activation process of the reaction on Ni anodes. The activation energy of the electrode polarization resistance for the reaction process at low frequencies ($R_{E,L}$) is 46 ± 9 kJ mol^{-1}, which is significantly lower than 102 ± 12 kJ mol^{-1} for the electrode process at high frequencies ($R_{E,H}$). For hydrogen oxidation on Ni/YSZ cermet anodes, the reaction can be separated into two rate-limiting electrode steps, namely, hydrogen dissociative adsorption and diffusion on the Ni surface and a charge-transfer reaction at the electrode and the YSZ electrolyte interface [14]. The electrode process associated with hydrogen adsorption and diffusion has a much lower activation energy than the charge-transfer process. The high value of $R_{E,H}$ observed in this study again indicates that the electrode process associated with high frequencies is a charge-transfer reaction at the TPB. This appears to be supported by the fact that the constant-phase element of the electrode process at the high-frequency arc (Q_H) is virtually independent of temperature. The n values (0.8–1) for the high-frequency arc are very close to 1, and therefore, Q_H can be approximated by the double-layer capacitance [14,15]. As the TPB area is determined primarily by the microstructure of the anodes, and in this case by the deposition and distribution of the impregnated YSZ, the double-layer capacitance associated with the TPB should not change significantly with temperature. On the other hand, the constant-phase element of the low-frequency arc (Q_L) varies considerably with temperature (Fig. 7b). This again indicates that the electrode process at the low-frequency arc is not be related to the charge transfer.

Nano-YSZ suspension impregnation treatment significantly enhances the microstructure and the electrode performance of Ni anodes for the hydrogen oxidation under SOFC operating conditions. The microstructure of the impregnated Ni anodes is characterized by very fine and uniformly distributed YSZ oxide particles on a continuous Ni network structure (Figs. 1 and 2). Low-temperature treatment of the ion impregnation process significantly reduces sintering and grain growth of the impregnated oxide phases. Cracium et al. [16] prepared Cu and Ni cermet anodes by impregnation of porous YSZ structure with Cu or Ni salt solutions and found that the Cu or Ni phase in the porous YSZ structure should be at least 40–50 vol.% to ensure adequate electrical conductivity and good performance. In the present approach, the anode is pre-fired at high temperatures

(1400 °C), and consequently, the Ni porous structure is stable and inherently electrically conductive. Thus, the impregnated oxide loading can be varied over a wide range without an adverse effect on the high electrical conductivity of the Ni anode. There is also no requirement on the minimum loading of the impregnated oxide phases. Thus, the electrode prepared by the impregnation method will have the combined advantages of high electrical conductivity of the Ni porous structure and high electrocatalytic activity of the impregnated oxides.

In the case of pure nickel anodes, the H_2 oxidation reaction will be limited to the TPB region as nickel is an electronic conductor with negligible oxygen ion conductivity [17] and oxygen must be transported to the reaction sites or to the TPB by solid diffusion through the YSZ phase. As hydrogen is a gaseous molecule, it can reach the TPB via adsorption and surface diffusion processes on YSZ or nickel or both surfaces. Despite the impregnation of nano-YSZ particles, the change in $R_{E,L}$ is very small compared with that for $R_{E,H}$ (Fig. 6). This in turn indicates that the YSZ surface may not be a good surface for dissociative adsorption of hydrogen. The nickel surface is probably preferred because hydrogen adsorbs dissociatively on nickel [18,19]. The activation energy of the electrode polarization at the low-frequency arc is $\sim$46 kJ mol^{-1}, close to the adsorption energy of 0.2–0.4 eV/molecule for dissociative adsorption of H_2 on nickel surfaces [18]. It is interesting to note that the measured activation energy for the electrode process at the low-frequency arc is close to the value of 0.425 eV/molecule proposed for the hydrogen dissociative adsorption on nickel by other workers [20]. This indicates that the electrode process at low frequencies may be dominated by dissociative adsorption of hydrogen YSZ impregnated Ni anodes even though the impedance information alone would not be sufficient to identify the exact nature of the electrode steps associated with the low frequencies. Additional supporting evidence is the observation that water in the system plays a significant catalytic role in the promotion of the surface diffusion process of hydrogen by the so-called 'spillover' mechanism [3,13]. This could significantly reduce the diffusion time of the hydrogen species compared with that of hydrogen adsorbates at regions close to the TPB.

4. Conclusions

The present study shows that impregnation of ionic conducting oxides, such as YSZ in the Ni anode significantly enhances the electrochemical activity for hydrogen oxidation. Impregnation of nano-YSZ not only substantially reduces the electrode interface resistance and the overpotential for the hydrogen oxidation reaction, but also clearly differentiates the electrode processes at low and high frequencies. Uniformly and discretely deposited nano-sized YSZ particles in Ni anodes simply extend the area of the three-phase boundary with no effect on the mechanism of hydrogen oxidation.

References

[1] B.C.H. Steele, Nature 414 (2001) 345.
[2] S.P. Jiang, S.H. Chan, J. Mater. Sci. 39 (2004) 4405.
[3] A. Bieberle, L.P. Meier, L.J. Gauckler, J. Electrochem. Soc. 148 (2001) 646.
[4] A. Bieberle, L.J. Gauckler, Z. Metallkd. 92 (2001) 7.
[5] S.P. Jiang, P.J. Callus, S.P.S. Badwal, Solid State Ionics 132 (2000) 1.
[6] M. Brown, S. Primdahl, M. Mogensen, J. Electrochem. Soc. 147 (2000) 475.
[7] S.P. Jiang, Y.Y. Duan, J.G. Love, J. Electrochem. Soc. 149 (2002) A1175.
[8] B. de Boer, M. Gonzalez, H.J.M. Bouwmeester, H. Verweij, Solid State Ionics 127 (2000) 269.
[9] S.P. Jiang, Y.J. Leng, S.H. Chan, K.A. Khor, Electrochem. Solid-State Lett. 6 (2003) A67.
[10] S.P. Jiang, S. Zhang, Y.D. Zhen, A.P. Koh, Electrochem. Solid-State Lett. 7 (2004) A282.
[11] S.P. Jiang, J. Mater. Sci. 38 (2003) 3775.
[12] S.P. Jiang, J. Electrochem. Soc. 150 (2003) E548.
[13] S.P. Jiang, S.P.S. Badwal, J. Electrochem. Soc. 144 (1997) 3777.
[14] S.P. Jiang, S.P.S. Badwal, Solid State Ionics 123 (1999) 209.
[15] S.P. Jiang, J.G. Love, S.P.S. Badwal, Key Eng. Mater. 125–126 (1997) 81.
[16] R. Cracium, S. Park, R.J. Gorte, J.M. Vohs, C. Wang, W.L. Worrell, J. Electrochem. Soc. 146 (1999) 4019.
[17] T.A. Ramanarayanan, R.A. Rapp, Metall. Trans. 3 (1972) 3239.
[18] T.N. Truong, D.G. Truhlar, B.C. Garrett, J. Phys. Chem. 93 (1989) 8227.
[19] A. Bieberle, L.J. Gauckler, Solid State Ionics 146 (2002) 23.
[20] R.E. Williford, L.A. Chick, G.D. Maupin, S.P. Simner, J.W. Stevenson, J. Electrochem. Soc. 150 (2003) A1067.